Available online at www.sciencedirect.com
ScienceDirect
Trans. Nonferrous Met. Soc. China 33(2023) 1594−1608
Transactions of Nonferrous Metals Society of China
www.tnmsc.cn

Preparation of vanadium electrolyte from vanadium shale leaching solution with high concentration chloride using D2EHPA

Hong LIU[1,2,3,4], Yi-min ZHANG[1,2,3,4], Tao LIU[1,2,3,4], Jing HUANG[1,2,3,4], Li-ming CHEN[1,2,3,4], You-wen HU[1,2,3,4]

1. College of Resource and Environmental Engineering, Wuhan University of Science and Technology, Wuhan 430081, China;
2. State Environmental Protection Key Laboratory of Mineral Metallurgical Resources Utilization and Pollution Control, Wuhan University of Science and Technology, Wuhan 430081, China;
3. Hubei Collaborative Innovation Center for High Efficient Utilization of Vanadium Resources, Wuhan University of Science and Technology, Wuhan 430081, China;
4. Hubei Provincial Engineering Technology Research Center of High Efficient Cleaning Utilization for Shale Vanadium Resource, Wuhan University of Science and Technology, Wuhan 430081, China

Received 29 November 2021; accepted 13 April 2022

Abstract: A process for preparing vanadium electrolyte accompanied by the recovery of valuable elements from vanadium shale was proposed. The results showed that under the optimal extraction conditions of the feed solution at a pH of 2.6, D2EHPA concentration of 20%, phase ratio (O/A) of 1:1, extraction time of 8 min, H_2SO_4 concentration of 4 mol/L, and stripping time of 30 min, the vanadium extraction rate was 99.3% and the vanadium stripping rate was 99.8%. The composition and electrochemical performance of the electrolyte were studied in detail. The solution chemical and FTIR analysis showed that chloride ions in the leaching solution formed complexes with vanadium ions, promoting vanadium extraction. The proposed method in this study realized the comprehensive utilization of vanadium shale and prevented toxic environmental pollution in the preparation process of vanadium electrolyte.
Key words: vanadium shale; solvent extraction; vanadium electrolyte; electrochemical performance

1 Introduction

With the consumption of fossil fuels and increasingly strict environmental protection policies, the development and utilization of renewable energy, such as wind and solar energy, has become urgent [1]. The all-vanadium flow battery is one of the most promising energy storage systems for commercial applications due to its long cycle life, no cross-contamination, fast response, deep discharge, and flexible location design [2−4].

The electrolyte preparation involves high-purity V_2O_5 (99.5%) as the raw material. However, a large number of reagents are consumed, especially in the process of vanadium precipitation. For instance, the use of excessive ammonium salts leads to high concentration ammonia nitrogen wastewater in the vanadium precipitation process, which increases the treatment cost and leads to environmental pollution [5,6]. In addition, numerous dissolution and precipitation cycles are needed to remove the various impurity ions. Vanadium shale, as an important vanadium-bearing resource, is a suitable raw material for electrolyte preparation as it contains less harmful elements such as Mn and

Corresponding author: Hong LIU, Tel: +86-27-68862057, E-mail: wustliuhong@126.com;
Yi-min ZHANG, Tel: +86-27-68862057, E-mail: zym126135@126.com
DOI: 10.1016/S1003-6326(23)66206-5
1003-6326/© 2023 The Nonferrous Metals Society of China. Published by Elsevier Ltd & Science Press

Cr. Therefore, shortening the process and reducing the generation of environmental pollutants are necessary, for instance, by obtaining vanadium electrolyte directly through purification and enrichment.

Solvent extraction technology is a highly efficient and selective process used for purification and enrichment. For the purification and enrichment of V(IV), organic phosphonic acid extractants are often used, including D2EHPA [7,8], PC88A [9,10], and Cyanex272 [11]. For V(V), amine extractants, such as primary amines, secondary amines and tertiary amines, have been most widely studied [12−15]. Chelating extractants have also been studied due to their excellent extraction performance and selectivity at low pH [16]. Among them, D2EHPA has been most widely used for V(IV) extraction in the industry due to its high extraction activity and low cost [17,18]. In addition, the vanadium-rich solution obtained from this system is a sulfuric acid solution mainly containing $VOSO_4$, which is a potential raw material for the vanadium redox flow battery (VRFB). Therefore, it is important to develop an efficient solvent extraction process to prepare the vanadium electrolyte from the vanadium shale leaching solution.

In this work, the process parameters of extraction and stripping were optimized and the extraction mechanism was studied. The performance of electrolyte was also characterized in detail. Additionally, Cr-rich and Na-rich slags were prepared from the raffinate. Compared with the traditional electrolyte preparation process, the generation of ammonium salt during the vanadium precipitation was prevented, and the vanadium electrolyte was achieved directly from the leaching solution.

2 Experimental

2.1 Chemicals and materials

The vanadium shale was supplied by Pingfan Mining Co., Ltd., Yunxi, Hubei Province, China, and the vanadium-rich leaching solution was prepared via roasting (7 wt.% Na_2CO_3, 3 wt.% NaCl, and 830 ℃) and water leaching technology. The chemical composition of the obtained vanadium shale leaching solution is listed in Table 1.

The analytical reagents, NaOH, H_2SO_4, Na_2SO_3, D2EHPA, and TBP, were supplied by the Sinopharm Group Co., Ltd., and were used without further purification.

Table 1 Main chemical composition of vanadium shale leaching solution (mg/L)

V	Si	Al	Fe	Ca	Mg	K
17728.9	288.7	5.1	4.0	224.1	150.3	5616.2
Na	Mn	P	Cr	Ni	Cu	Mo
43430.1	1.9	93.91	1094.1	<1	<1	108.3
As	Au	Pt	Pd	Cl	SO_4^{2-}	
10.5	<1	<1	<1	31187.5	63867.5	

2.2 Methods

2.2.1 Solvent extraction

The solvent extraction experiment was carried out in a 100 mL beaker at 25 ℃. The stirring speed was 250 r/min. The organic phase was composed of 20 vol.% D2EHPA as the extractant, 5 vol.% TBP as the phase modifier and 75 vol.% sulfonated kerosene as the diluent. The pH of the feed solution was adjusted by 6 mol/L HCl and 10 mol/L NaOH solutions. Each experiment was performed three times to obtain accurate and reproducible data.

2.2.2 Electrochemical measurements

A three-electrode system was used for electrochemical testing, with a graphite electrode (1 cm × 1 cm) as the working electrode, a platinum electrode (2 cm × 2 cm) as the counter electrode, and a saturated calomel electrode as the reference electrode.

Cyclic voltammetry (CV) tests were conducted within a potential range of 0.4−1.4 V at a scan rate of 10 mV/s. The electrochemical impedance spectroscopy (EIS) test was carried out on a CHI660E electrochemical workstation. The results were fitted with a simplified equivalent electric circuit model.

2.2.3 Charge−discharge tests

Firstly, the V(IV) electrolyte was placed into the positive and negative electrode storage tanks at a volume ratio of 2:1. After the preliminary charging was completed, the electrolyte in the positive and negative electrode storage tanks consisted of V(V) and V(II), respectively. Half of the electrolyte was poured into the positive electrode storage tank, and the charge−discharge tests were performed. The cell performance was measured on a CT2001B−5V/10A battery test

system (Wuhan Land Co., Ltd., China) at a constant current density of 40 mA/cm within a potential range of 0.65−1.65 V. The electrolyte was circulated through a peristaltic pump, and the flow rate was set to the 40 mL/min. After the charge−discharge test, the coulombic efficiency, voltage efficiency and energy efficiency were calculated.

2.2.4 Instruments and analysis

The pH value was measured on a pH meter (PHS−3C, supplied by Shanghai INESA). The concentration of vanadium ions in the solution was determined by titration method (GB/T 8704.5—2007, China). UV−Vis spectrometry measurement of the prepared vanadium electrolyte was carried out on a UNIC 4802S UV−Vis spectrophotometer (Shanghai, China). The composition of the solution was analyzed by inductively coupled plasma atomic emission spectrometry (ICP-AES). The oxidation states of the V ions at different pH values, as shown in Fig. 1, were calculated by the thermodynamic software Visual Minteq 3.1. The main indicators and calculation methods are shown in Eqs. (1)−(3):

$$D=\frac{C_{\text{org}}}{C_{\text{aq}}} \tag{1}$$

$$\eta=\frac{D}{D+(V_{\text{aq}}/V_{\text{org}})}\times 100\% \tag{2}$$

$$\beta_{\text{a,b}}=\frac{D_{\text{a}}}{D_{\text{b}}} \tag{3}$$

where C_{aq} and C_{org} are the ion concentrations in the feed solution and organic phases, respectively, η is the extraction rate, D is the ratio of ion concentration in the organic phase to that in feed solution phase, $\beta_{\text{a,b}}$ is the separation coefficient of vanadium and the impurity ions, and V_{aq} and V_{org} are the volumes of the feed solution and organic phase, respectively.

3 Results and discussion

3.1 Pretreatment of vanadium shale leaching solution

The existing form of vanadium in the feed solution is known to have a strong impact on the extraction efficiency [19]. According to Table 1, the leaching solution contained a large number of chloride ions. Previous studies [20,21] have shown that the chloride ion has a strong coordination ability; therefore, the oxidation states of the vanadium ions need to be studied first. Figure 1(a) shows that V(V) anions are found under acidic and neutral pH conditions. It is worth noting from Fig. 1(a) that Na^+ and K^+, which may be introduced during solvent extraction, easily form complex ions with vanadium. Figure 1(b) shows that chloride ions can be complexed with vanadium ions, and that vanadium exists mainly in the form of $VOSO_4$, $VOCl^+$, and VO^{2+} under acidic conditions, which can be theoretically extracted with D2EHPA by cation exchange. Therefore, Na_2SO_3 was used to reduce the vanadium leaching solution [22], and the mass of Na_2SO_3 was two times the theoretical requirement. Thus, the reduction solution was obtained.

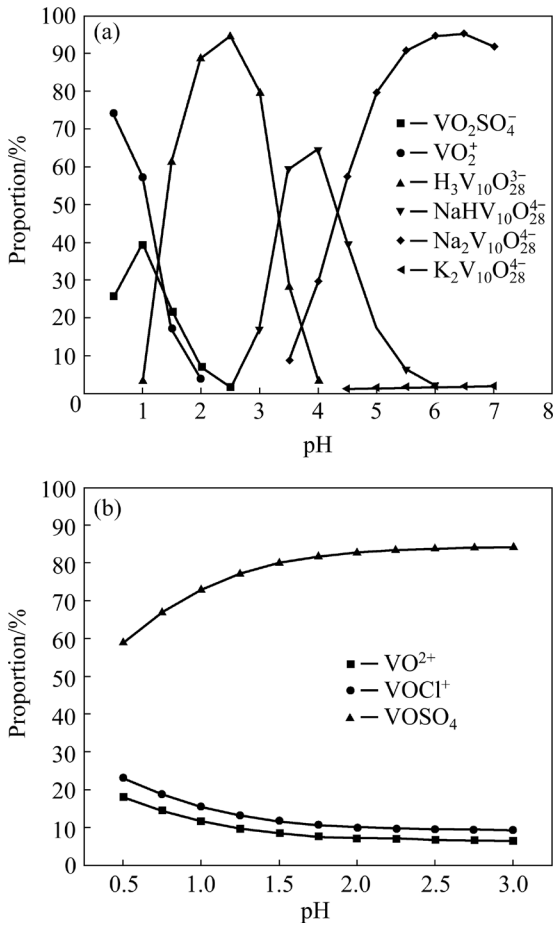


Fig. 1 V(V) (a) and V(IV) (b) ions found in feed solution

The primary and reduction solutions, i.e., Solutions A and B, respectively, obtained from the vanadium shale leaching solution, were studied by UV−Vis spectrometry, as shown in Fig. 2. Solution A shows a series of miscellaneous peaks from 200 to 400 nm, which are the characteristic peaks of V(V). After the reduction, Solution B shows one

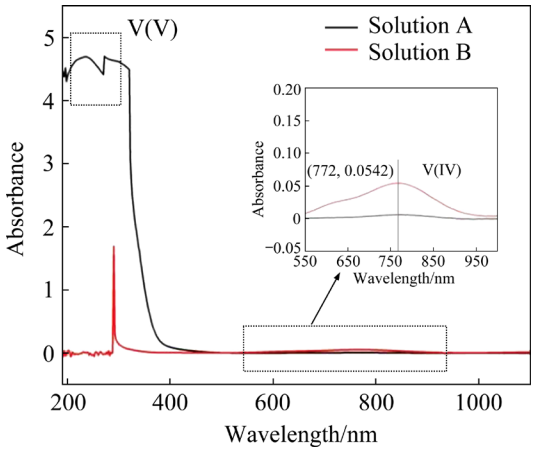


Fig. 2 UV−Vis spectra for primary vanadium shale leaching solution (Solution A) and vanadium shale leaching solution after reduction (Solution B)

characteristic absorption peak at 772 nm, which is the characteristic peak of the V(IV) ion [23,24]. Thus, mainly pentavalent vanadium is found in the leaching solution, which is related to the oxidizing roasting process [25]. The results also show that Na_2SO_3 could effectively reduce V(V) to V(IV).

3.2 Preparation of vanadium electrolyte

3.2.1 Extraction

The effects of pH, D2EHPA concentration, phase ratio, and extraction time on the vanadium extraction were investigated, as shown in Fig. 3.

The pH of the feed solution had a significant impact on the vanadium extraction. It was found that a blue precipitate was easily obtained when the pH value of the feed solution exceeded 3. Therefore, the effect of the feed solution pH, from 1.8 to 2.8, on the vanadium extraction was studied, as shown in Fig. 3(a). The vanadium extraction rate slowly increased from 1.8 to 2.2 and plateaued from 2.2 to 2.8. In the D2EHPA−vanadium extraction, previous studies [26,27] showed that the extraction reaction released hydrogen ions, indicating that an increase in pH was conducive to the forward reaction of extraction. In this study, the pH value of the leaching solution was neutral, so a pH value of 2.6 was selected as the optimal point, which prevented the precipitation of V(IV) and reduced the reagent consumption in the pH adjustment process.

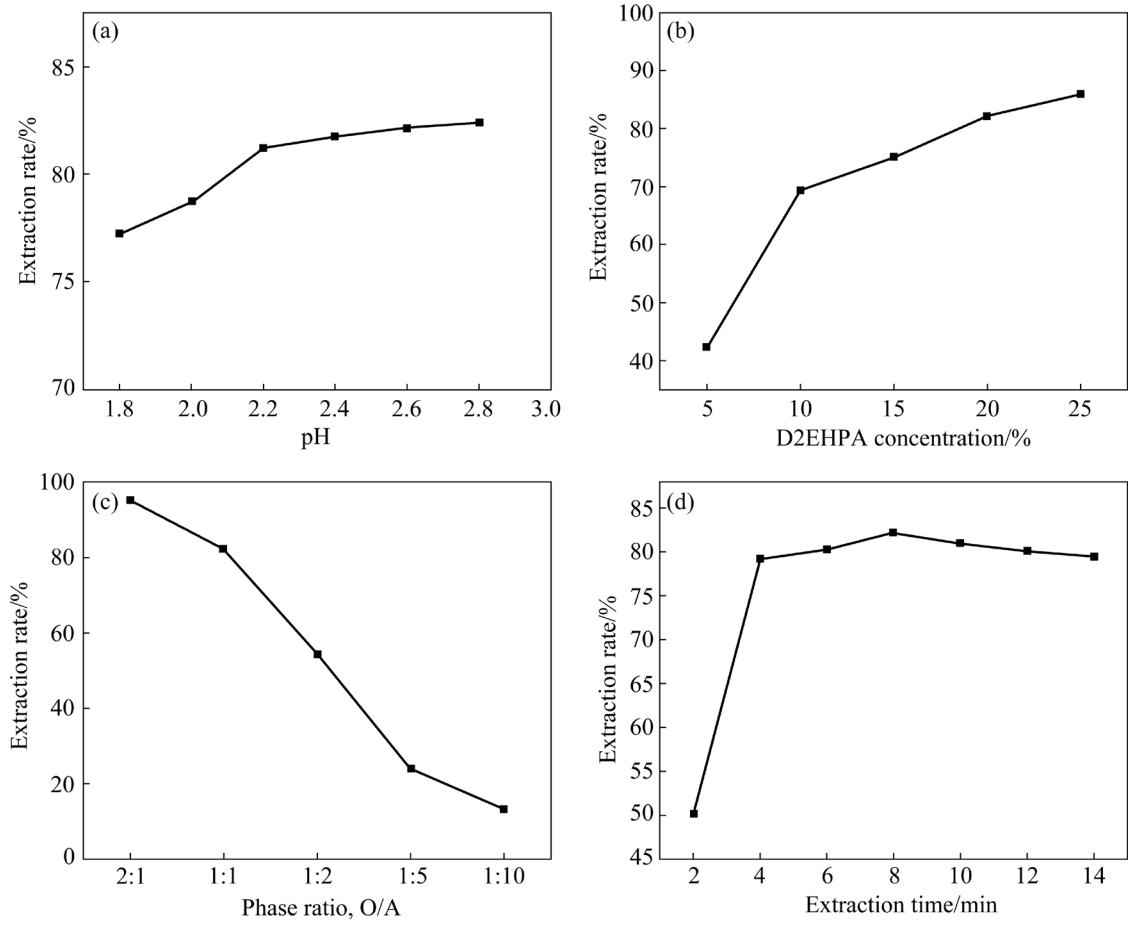


Fig. 3 Effects of pH (a), D2EHPA concentration (b), phase ratio (c), and extraction time (d) on vanadium extraction rate

As a reactant with vanadium ions, the concentration of the extractant plays an important role in the extraction process and can be divided into two stages, as shown in Fig. 3(b). The extraction rate of vanadium showed a rapid increase in the extractant concentration range of 5%−10%. When the concentration of the vanadium extractant was greater than 10%, the extraction rate slowly increased. However, the viscosity of the organic phase tended to increase with the extractant concentration, which can lead to large mass transfer resistance. Therefore, the optimal extractant concentration was determined to be 20% in the subsequent experiments.

Phase ratio plays an important role in the solvent extraction, as it largely determines the enrichment ratio of vanadium ions and rate efficiency. The influence of the phase ratio (O/A) on the vanadium extraction is shown in Fig. 3(c). The vanadium extraction rate showed a significant decrease with the decrease in phase ratio, particularly when the phase ratio was lower than 1:1. Since the initial vanadium concentration of the feed solution in this study reached 16 g/L, further enrichment of vanadium could be achieved in the subsequent stripping process. The main task in the extraction process was to separate vanadium from the impurity ions. Therefore, the optimal phase ratio (O/A) was selected to be 1:1.

The effect of extraction time on vanadium extraction is shown in Fig. 3(d). The vanadium extraction rate increased from 50.20% to 79.20% when the mixing time increased from 2 to 4 min. Above 4 min, the vanadium extraction rate showed a slight upward, followed by a downward trend. The highest extraction rate was 82.15% at 8 min. Long duration extraction may lead to an increase in co-extraction of impurity ions; therefore, the best extraction time was found to be 8 min.

According to the above mentioned results, the optimal conditions for the extraction process involved a feed solution with a pH of 2.6, D2EHPA concentration of 20%, phase ratio (O/A) of 1:1, and extraction time of 8 min. Under these conditions, the vanadium single-stage extraction rate was 82.15%. To determine the number of extraction stages in the counter-current experiment, the extraction isotherm was studied under optimal conditions. The McCable−Thiele diagram was drawn by the variable phase method, as shown in Fig. 4. Thus, theoretically, three levels were required to reduce the vanadium concentration from 15.956 to 0.15 g/L, for a vanadium extraction rate greater than 99%. However, an additional stage was required in the actual operation process to ensure the extraction rate. After 4 stages of counter-current solvent extraction, an organic phase containing 15.8 g/L vanadium was obtained, and 99.3% of vanadium was extracted. Then, the organic phase was washed with water for 5 min, with an O/A ratio of 2:1, in two stages. Thus, the inclusions in the organic phase were washed, and no vanadium was lost.

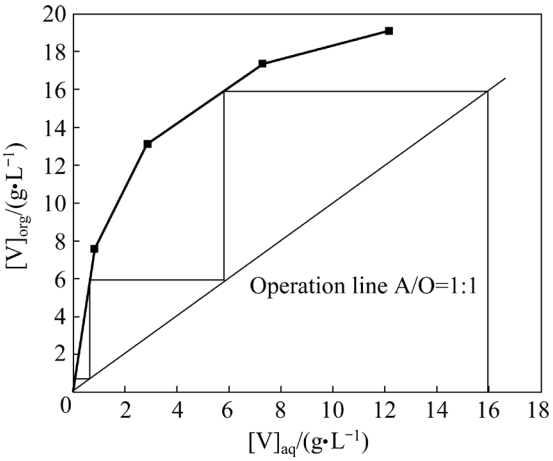


Fig. 4 McCable−Thiele plot for vanadium extraction

3.2.2 Stripping

In the extraction process, vanadium was separated from the main impurity ions, but it was necessary to further enrich vanadium by the stripping process. For this purpose, the physical and chemical properties of the stripping solution should meet the requirements of the electrolyte. Studies show that the vanadium concentration of the conventional electrolyte needs to be greater than 1.6 mol/L [28]. The obtained vanadium concentration in the stripping solution met the requirements of the electrolyte theoretically when the calculated phase ratio (O/A) was 6:1. Sulfuric acid was selected as the stripping agent since most existing electrolytes used sulfuric acid as a medium. Additionally, the impact of the sulfuric acid concentration and stripping time on the stripping rate was investigated, as shown in Fig. 5.

Figure 5(a) shows that the vanadium stripping rate increased from 56.55% to 79.00% while increasing the H_2SO_4 concentration from 2 to 3 mol/L. The vanadium stripping rate presented a

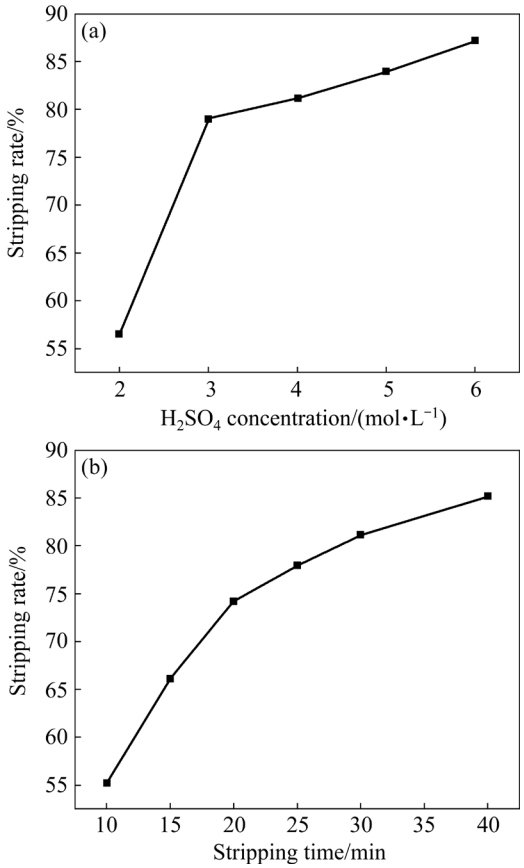


Fig. 5 Effects of H_2SO_4 concentration (a) and stripping time (b) on vanadium stripping rate

slow upward trend when the H_2SO_4 concentration was more than 3 mol/L. To ensure the concentration of hydrogen ions and sulfate ions in the electrolyte, 4 mol/L sulfuric acid was selected as the stripping agent concentration.

The impact of stripping time is shown in Fig. 5(b). The stripping rate of vanadium showed an upward trend with the extension of the stripping time. To improve the stripping efficiency, 30 min was chosen as the optimal stripping time, and an 81.15% single-stage stripping rate was achieved.

The McCable−Thiele diagram of vanadium counter-current extraction was drawn by the variable phase method at 4 mol/L H_2SO_4, and a stripping time of 30 min, as shown in Fig. 6. Theoretically, vanadium concentration in the organic phase could be reduced below 50 mg/L through two-stage stripping. During actual operation, a vanadium stripping rate of 99.80% could be obtained through three-stage stripping. After stripping, the organic phase was regenerated by two-stage counter-current washing with 20% sulfuric acid and one-stage water washing to obtain

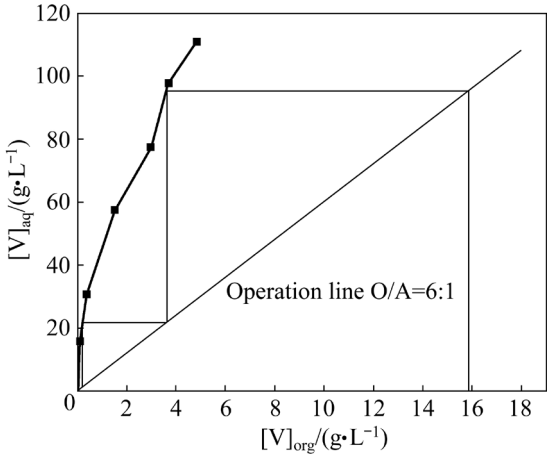


Fig. 6 McCable−Thiele plot for vanadium stripping

a regenerated organic phase, which was used for circulating the extractant.

3.2.3 Separation performance

To study the separation performance of vanadium and impurity ions in the extraction and stripping processes, the compositions of the feed solution, raffinate and vanadium-rich solutions are shown in Table 2. The separation of vanadium and most of the impurity ions in the leachate was effective. The vanadium concentration in the vanadium-rich solution obtained by the extraction method reached 1.77 mol/L, which met the requirement of vanadium concentration in common electrolytes. However, it is not clear if the performance of the electrolyte is impacted by trace amounts of impurities; thus, necessitating further studies.

3.2.4 Extraction mechanism

The fresh organic phase and the loaded organic phase were analyzed by FTIR to study the vanadium extraction mechanism, as shown in Fig. 7. The peaks at 2336.79, 2731.25, 1235.05, and 1034.73 cm^{-1} are attributed to the stretching vibration of hydrogen bond-associated P—O—H bond, bending vibration of hydrogen bond-associated P—O—H bond, associated P═O bond coupling vibration and P — O — C vibration, respectively [29,30]. After vanadium extraction, the stretching and bending vibrations of the P—O—H bond shifted to 2317.49 and 2730.62 cm^{-1}, respectively. The characteristic peak of coupling vibration of P═O bond shifted to 1231.69 cm^{-1}, while the shift of the characteristic peak for P—O—C was not significant. The FTIR analysis showed that the vanadium extraction mechanism in

Table 2 Compositions of raffinate and vanadium-rich solutions (mg/L)

Sample	V	Si	Al	Fe	Ca	Mg	K
Feed solution	15956.3	229.9	2.8	1.6	179.1	124.9	3715.1
Raffinate	111.7	226.9	2.0	0.8	173.5	123.6	3704.0
Vanadium-rich solution	90093.3	11.3	4.6	2.7	21.7	1.7	48.8
Sample	Na	Mn	P	Cr	Ni	Cu	Mo
Feed solution	59758.1	1.8	89.2	793.1	<1	<1	29.9
Raffinate	59676.0	1.6	86.1	791.4	<1	<1	28.3
Vanadium-rich solution	468.8	<1	12.7	<1	<1	<1	<1
Sample	As	Au	Pt	Pd	Cl		
Feed solution	6.5	<1	<1	<1	65199.7		
Raffinate	6.3	<1	<1	<1	63472.5		
Vanadium-rich solution	<1	<1	<1	<1	10195.0		

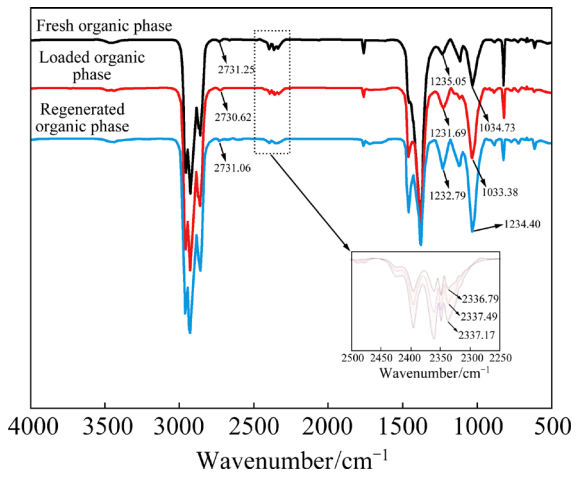


Fig. 7 FTIR spectra of fresh, loaded and regenerated organic phases

this system was similar to that in the sulfuric acid system, which involves the exchange of H^+ and vanadium ions. However, in this study, in addition to sulfate ions, there were also a large number of chloride ions in the feed solution; thus, a considerable part of vanadium exists as $VOCl^+$. Therefore, the main chemical reactions that are expected to occur during the extraction process are shown in Reactions. (4) and (5), and the possible forms of vanadium complexes with D2EHPA are demonstrated in Fig. 8.

$$VO^{2+}_{(aq)} + 2(HA)_{2(org)} = VOA_2 \cdot (HA)_{2(org)} + 2H^+_{(aq)} \quad (4)$$

$$VOCl^+_{(aq)} + (HA)_{2(org)} = VOClA \cdot (HA)_{(org)} + H^+_{(aq)} \quad (5)$$

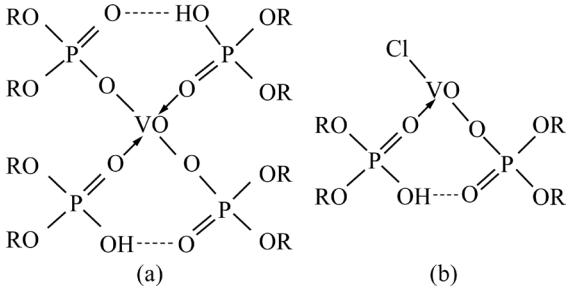


Fig. 8 Possible vanadium complexes formed with D2EHPA

Figure 7 also shows that the main characteristic peaks of the infrared spectra of the regenerated organic phase were similar to those of the fresh organic phase, indicating that the regeneration process achieved the regeneration of D2EHPA.

3.3 Performance of vanadium electrolyte

3.3.1 Cyclic voltammetry

Cyclic voltammetry (CV) was used to study the electrochemical activity and electrochemical reversibility of the V(IV) electrolyte sample prepared from the vanadium shale. To better understand the performance of the experimental electrolyte (EE), the standard electrolyte (SE) was prepared as the control group. The concentrations of the vanadium ion and sulfuric acid in the SE were consistent with those in the EE, as shown in Fig. 9(a). The oxidation peak current density (J_{pa}), reduction peak current density (J_{pc}), oxidation peak potential (φ_{pa}), reduction peak potential (φ_{pc}) and peak potential difference ($\Delta\varphi_p$) were obtained from the CV results, as shown in Table 3.

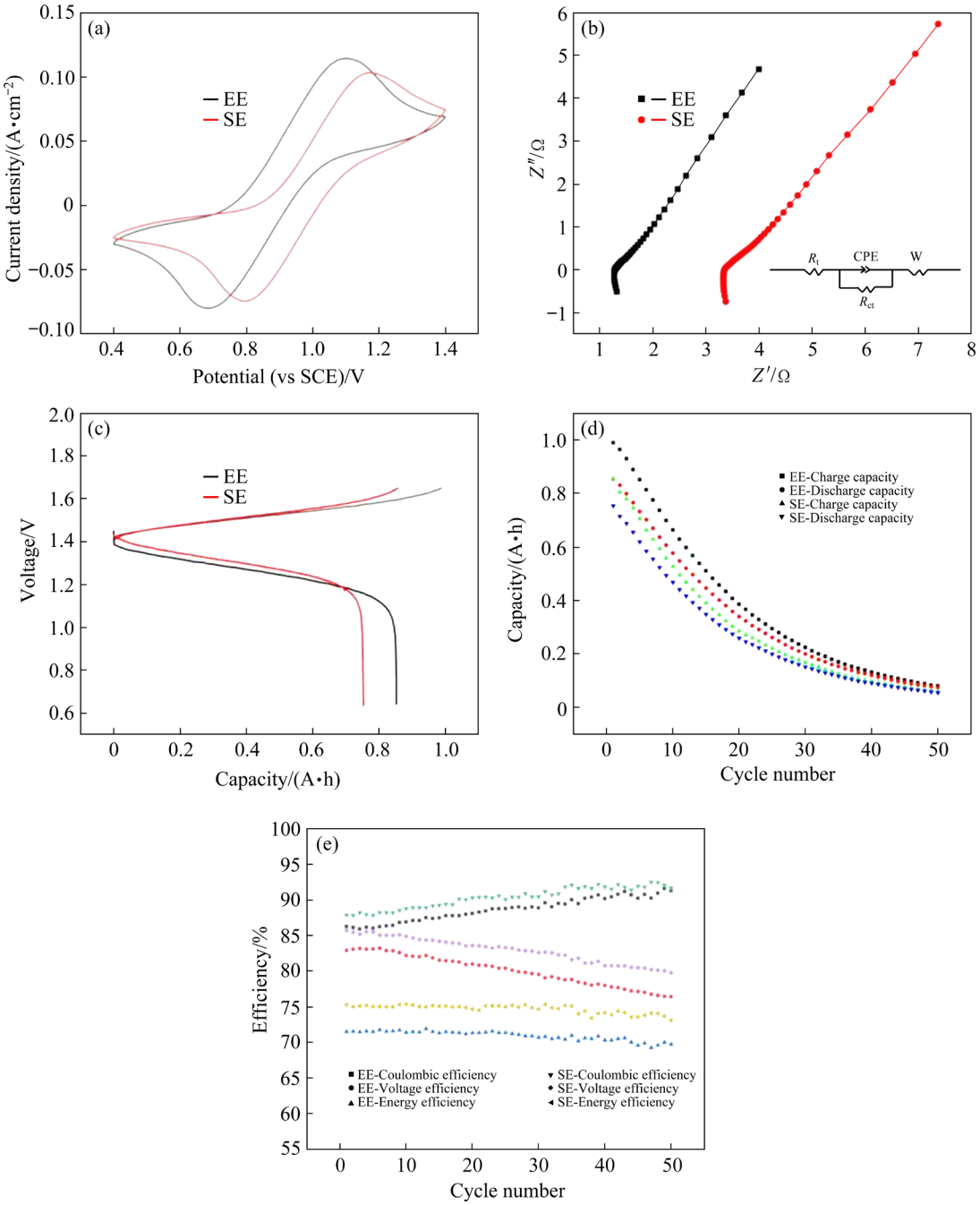


Fig. 9 CV curves (a), Nyquist plots and equivalent electric circuit model (b), Charge−discharge curves at the 1st cycle (c), capacity change of VRFB in 50 cycles (d), and coulombic, voltage and energy efficiency (e) of EE and SE

Table 3 Parameters of CV tests for experimental electrolyte (EE) and standard electrolyte (SE)

Sample	Oxidation peak		Reduction peak		$\Delta\varphi_p$/V	J_{pa}/J_{pc}
	J_{pa}/(mA·cm^{-2})	φ_{pa}(vs SCE)/V	J_{pc}/(mA·cm^{-2})	φ_{pc}(vs SCE)/V		
EE	114.40	1.098	79.95	0.685	0.413	1.43
SE	103.20	1.166	74.47	0.796	0.370	1.39

Figure 9(a) showed that the CV curves of EE and SE presented a symmetrical shape, indicating electrochemical reversibility. Table 3 showed that the value of J_{pa}/J_{pc} for EE was closer to 1, implying that the reversibility of SE was better than that of EE. In addition, the current densities of the

oxidation and reduction peaks of EE were higher than those of SE, indicating that the corresponding redox reaction on the surface of the electrode was kinetically favorable. The CV test involved a three-electrode system, where the working electrode was a graphite electrode, and the potential difference with SE was 1.39 V, which was mainly affected by the graphite electrode. Under the same test conditions, the potential difference of EE increased, which may be mainly affected by impurity ions. There were still trace amounts of impurity ions in the electrolyte prepared in this experiment. Impurity ions can increase the current density of the electrolyte to a certain extent, but also reduce the reversibility of the electrolyte. Compared with the SE electrolyte, EE had higher current densities of oxidation and reduction peaks, and the overall CV curve shifted towards the left, indicating that EE had a faster redox reaction, suggesting better capacity and higher efficiency.

3.3.2 Electrochemical impedance spectroscopy

EIS was used to analyze the electrode reaction kinetics of the EE and SE, as shown in Fig. 9(b). The EIS curves were composed of a semicircular arc in the high-frequency region and a straight line in the low-frequency region, indicating that the V(IV)/V(V) oxidation−reduction reaction process in the electrolyte was jointly controlled by the mass transfer and charge transfer processes. As the frequency decreased, the ion diffusion resistance increased and since the ions at the interface tended to adsorb the same number of electrons, the low-frequency region in the Nyquist spectrum was a 45° straight line.

The electrode reaction kinetic parameters of EE and SE were fitted by the corresponding equivalent circuit model. The fitting values of the solution resistance (R_1), the charge transfer resistance (R_{ct}), the electric double-layer capacitance (C), of the electrode/solution interface, and the diffusion resistance (W) are shown in Table 4. The R_1 in EE was lower, while R_{ct} and W were higher than those in SE. As a result, the solution impedance and charge transfer resistance of the EE electrolyte were larger, which led to an increase in the electrochemical polarization of the electrolyte and a severer side reaction on the electrode surface. Compared with SE, the increase in R_{ct} and W of EE tended to be affected by the increase in electrolyte viscosity. The viscosity of EE (4.42 mm^2/s) was higher than that of SE (4.34 mm^2/s), indicating that the electrolyte prepared from shale had a slower charge transfer rate and diffusion rate. Combined with the viscosity test, it was found that the viscosity of EE was relatively large, which might be mainly affected by impurity ions in the electrolyte. A previous study [31] showed that a small amount of impurity ions in the electrolyte might had a favorable effect on the electrochemical performance of the electrolyte.

Table 4 Fitting results of EIS obtained from equivalent circuit

Sample	R_1/ ($\Omega\cdot cm^{-2}$)	C/ (10^{-2} $F\cdot cm^{-2}$)	R_{ct}/ ($\Omega\cdot cm^{-2}$)	W/ ($S\cdot s^{1/2}\cdot cm^{-2}$)
EE	1.259	5.344	7.064	0.1536
SE	3.348	5.271	5.477	0.1022

3.3.3 Charge–discharge performance

As the active material of the VRFB, the performance of the electrolyte also impacts the performance of the VRFB. Therefore, the electrolyte prepared from the vanadium shale leaching solution was evaluated through charge−discharge battery performance tests to determine its applicability in VRFB. The efficiency of the vanadium battery can be affected by many aspects, such as the electrolyte, electrode and battery structure. In this study, the same single-cell system and test conditions for EE and SE, such as current density and flow rate, were selected to reduce error. The main reason for the decrease in the capacities and efficiencies of SE and EE after multiple charge−discharge cycles was the migration of the electrolyte. It was found that SE had a greater capacity loss in this test system, indicating that this was not caused by the electrolyte itself. It might be affected by the single-cell system and membrane, resulting in an imbalance in the volume and concentration of the positive and negative electrolytes, thereby affecting its charge−discharge performance. Excluding the influence of the system, the detailed comparison results of the charge and discharge performance of the EE and SE are described as follows.

To study the cycle performance for the battery efficiency, the charge−discharge curve and capacity change of EE and SE were studied, as shown in Figs. 9(c) and (d). As shown in Fig. 9(c), the EE and SE initially had a lower charging voltage

platform and a higher discharge voltage platform, and the charging and discharging capacities were higher. As shown in Fig. 9(d), as the number of cycles increased, the charge and discharge capacities of the battery decreased significantly. The charge and discharge capacities for EE, in the first cycle, were 0.989 and 0.853 A·h, respectively, and the charge and discharge capacity retention rates after 50 cycles were 8.09% and 8.56%, respectively. The charge−discharge capacities for SE in the first cycle were 0.857 and 0.753 A·h, respectively. The charge−discharge capacity retention rates after 50 cycles were 7.00% and 7.30%, respectively. Thus, the electrolyte obtained by the extraction method showed a good charge−discharge capacity, and the capacity retention rate was consistent with that of the standard electrolyte.

The coulombic, voltage and energy efficiencies of the battery during 50 cycles are shown in Fig. 9(e). As the number of cycles of charge and discharge increased, the coulomb efficiency presented a slight upward trend, the voltage efficiency showed a slight downward trend, while the energy efficiency remained stable. The coulombic, voltage and energy efficiencies of the first cycle for EE were 86.25%, 82.90% and 71.50%, respectively. Across all the charge−discharge cycles, the average coulombic efficiency, voltage efficiency and energy efficiency for EE were 88.65%, 80.06%, and 70.93%, respectively. The coulombic, voltage and energy efficiencies of the first cycle for SE were 87.86%, 85.70% and 75.30%, respectively. Across all the charge−discharge cycles, the average coulombic, voltage and energy efficiencies for SE were 90.28%, 82.92% and 74.71%, respectively.

These results indicate that the prepared electrolyte exhibited good electrochemical performance during the actual operation of the VRFB. The oxidation and reduction peak current densities, solution resistance and charge−discharge capacity of the prepared electrolyte were superior to those of standard electrolytes. These advantages can be attributed to the coordination effect of a large number of chloride ions in electrolytes. Previous studies [32−34] have shown that the addition of different concentrations of chloride ions in the electrolyte could effectively improve the electrochemical reaction on the electrode surface and the performance of the electrolyte. In this study, chloride ions were extracted into the electrolyte in the solvent extraction process. The introduction of chloride ions resulted in vanadium−chloride mononuclear or binuclear complexes, which could effectively reduce the vanadium ion cross-over, reduce battery capacity loss and improve efficiency. To avoid the corrosive effect of chloride ions, reactors are composed of anti-corrosion materials in the industry. In addition, no significant chlorine volatilization was observed in this study, but in the industry it is necessary to control the charging cut-off voltage to prevent the release of harmful chlorine gas.

3.4 Recovery of valuable elements and establishment of separation flow chart

According to the results in Section 3.2.4, vanadium was effectively recovered and high-value utilization for VRFB was realized through the solvent extraction process. However, hazardous but valuable ions were still present in the raffinate, such as Cr and Na ions. SHI et al [35] have shown that Cr ions in water are toxic to the environment, and high concentration of Na ions is one of the main reasons for wastewater with high salt content [36]. Therefore, it is necessary to further process the raffinate and recover valuable elements; thus, the process is environmentally friendly, and provides by-products to save costs.

After Na_2SO_3 reduction, mainly trivalent chromium was found in the solution [37]. Chemical precipitation is an effective method to remove trivalent chromium ions. On adjusting the pH value of the raffinate to 7 with 10 mol/L NaOH, after 1 h of reaction at room temperature, a green powder was obtained. The XRD patterns and SEM−EDS analysis results of the by-product are shown in Fig. 10.

Figure 10(a) showed that the XRD pattern of the precipitate mainly contained a dispersion peak, indicating that the precipitate was not crystalline. In addition, the characteristic peaks of NaCl could be seen, suggesting that the chloride and sodium ions in the solution were entrained into the precipitate. Further SEM−EDS analysis (Fig. 10(c)) of the precipitates showed that the precipitates mainly contained Cr, and showed good consistency with the O. Previous studies [38,39] indicated that Cr was mainly precipitated in the form of $Cr(OH)_3$. Additionally, a large amount of vanadium was found

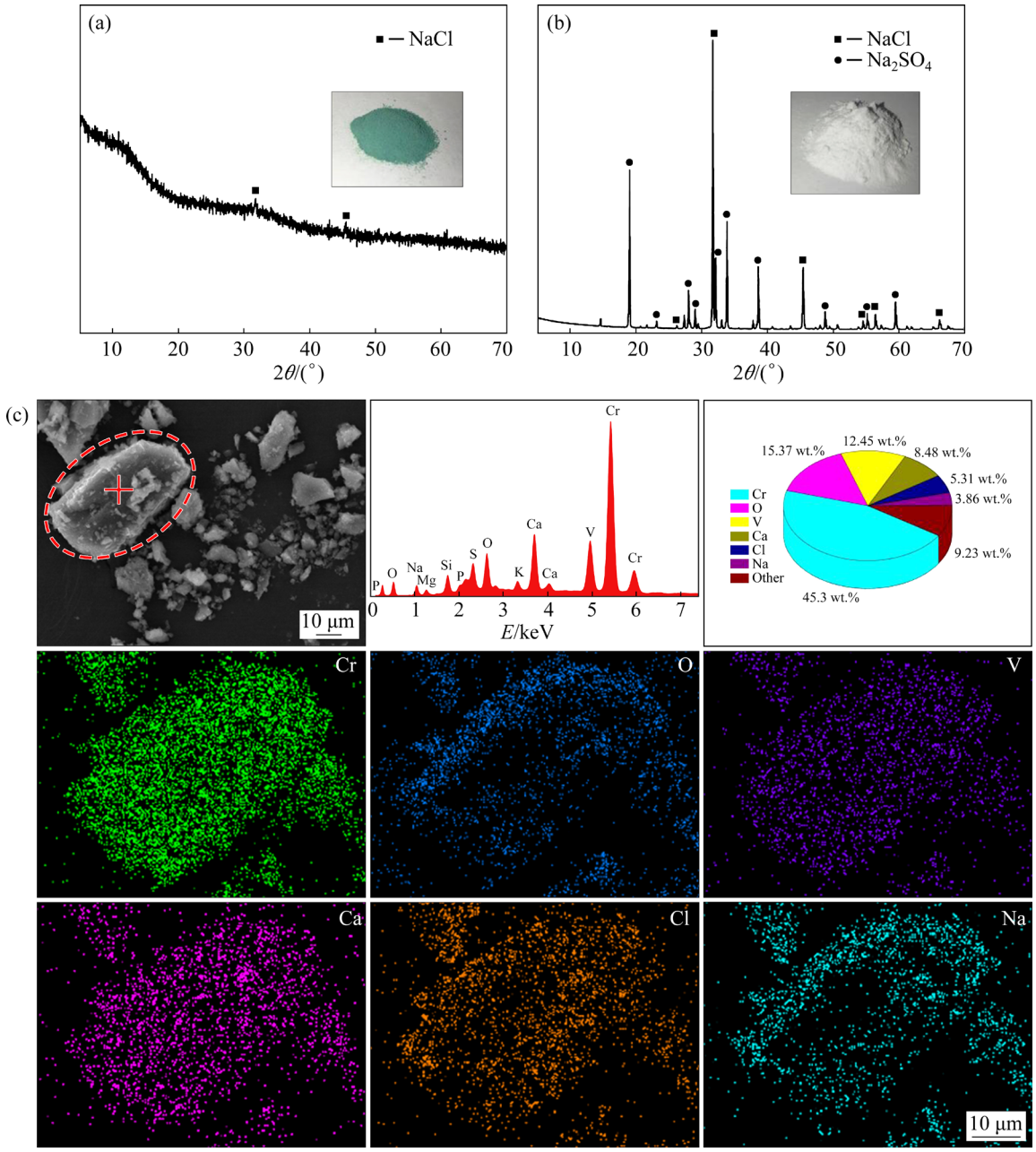


Fig. 10 Analysis results of by-products: (a) XRD pattern of Cr-rich sediment; (b) XRD pattern of Na-rich sediment; (c) SEM−EDS data of Cr-rich sediment

in the precipitate, which can be attributed to the precipitation of V(IV) ions in the form of VO_2 during the pH adjustment process. EDS analysis showed that the Cr content reached 45.3 wt.%, in which chromium-rich slag could be used as raw material for the preparation of chromium products. The main chemical reactions that occur in this process are shown in Reactions (6) and (7):

$$Cr^{3+}+3OH^{-}\rightarrow Cr(OH)_3\downarrow \quad (6)$$

$$VO^{2+}+H_2O\rightarrow VO_2\downarrow+2H^{+} \quad (7)$$

Thus, Cr was removed from the raffinate and the removal rate was 99.6%. By evaporating and crystallization of the residual liquid, a white solid was obtained. The XRD results in Fig. 10(b) indicate that the crystals mainly consisted of NaCl and Na_2SO_4, which could be used as additives in the roasting process.

Based on the above mentioned results, an ultra-short and eco-friendly process for preparing vanadium electrolyte, accompanied by the recovery of valuable elements, was established in Fig. 11. In this schema, firstly, selective extraction and stripping were achieved using D2EHPA. Most of the impurities

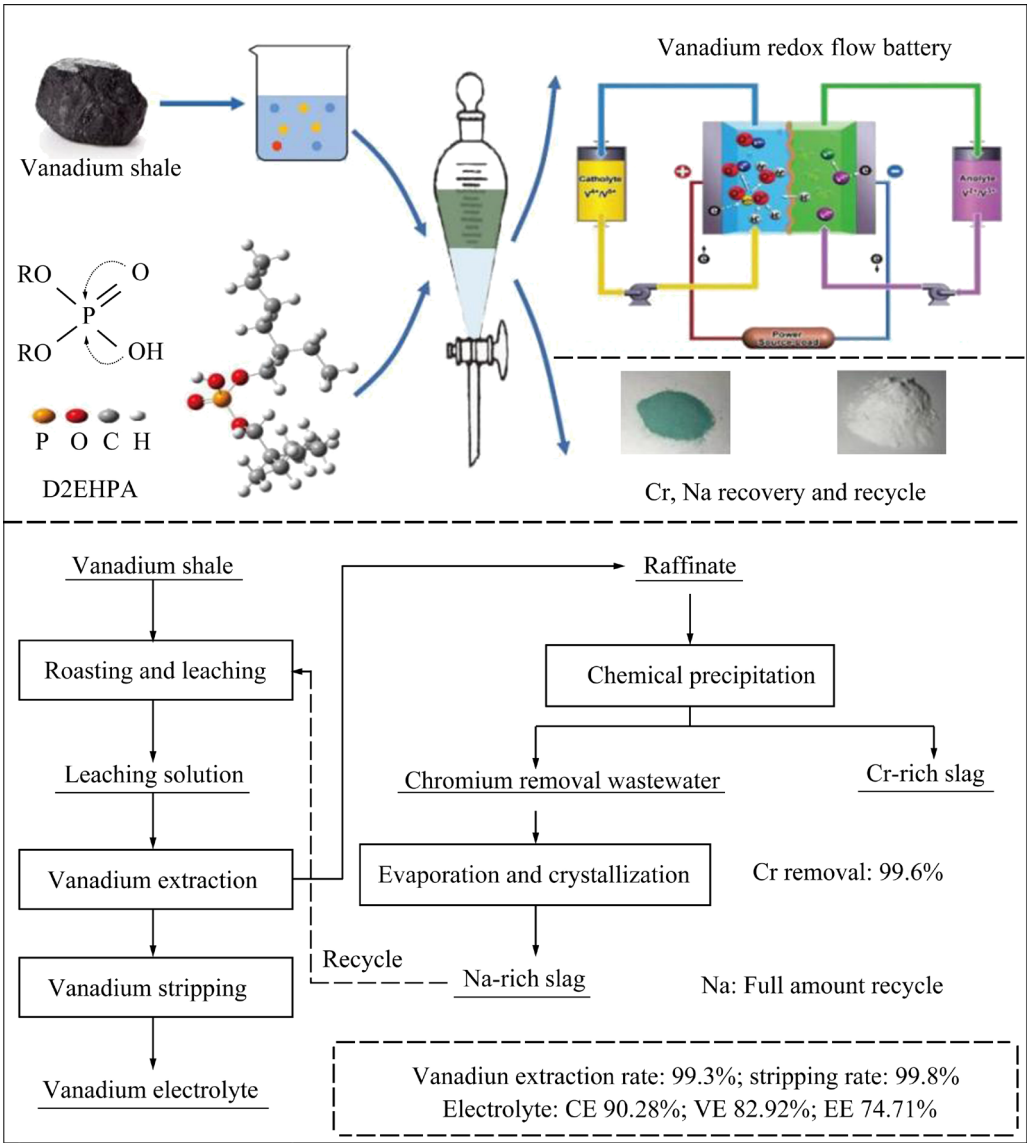


Fig. 11 Ultra-short and eco-friendly process for preparing vanadium electrolyte accompanied by recovery of valuable elements

were separated and high value-added electrolyte was obtained from the vanadium shale leaching solution. Then, the chromium ion was recovered by the chemical precipitation method to obtain the chromium-rich slag. Finally, the remaining liquid was concentrated and crystallized to obtain a mixture of sodium chloride and sodium sulfate, which could be used as additives in the roasting process.

Compared with the traditional preparation process for electrolytes, this process avoided the generation of ammonium salt in the vanadium precipitation process, and realized the preparation of the vanadium electrolyte directly from the leaching solution. In addition, the Cr and Na ions in the raffinate were also recovered, which avoided the generation of potential hazards to the environment.

4 Conclusions

(1) Under the optimal extraction condition of the feed solution, with a pH of 2.6, D2EHPA concentration of 20%, phase ratio of 1:1, and extraction time of 8 min, the vanadium extraction rate was 99.3%. Under the optimal stripping condition of 4 mol/L H_2SO_4 and stripping time of 30 min, the vanadium stripping rate was 99.8%. The separation of vanadium from the main impurity ions was achieved. Solution chemistry and FTIR analyses indicate that the chloride ions can form

complexes with vanadium ions in the feed solution, promote vanadium extraction, and finally enter the electrolyte in the stripping process.

(2) The electrolyte prepared from the vanadium shale exhibited good electrochemical performance in the electrolyte and battery tests. The CV, EIS and charge−discharge tests indicated that the oxidation and reduction peak current densities, solution resistance and charge−discharge capacity of the prepared electrolyte were superior to those of standard electrolytes. The average coulombic, voltage and energy efficiencies for EE were 90.28%, 82.92% and 74.71%, respectively.

(3) Cr was precipitated in the form of $Cr(OH)_3$, and Na was recycled as NaCl and Na_2SO_4, which can be used as roasting additives for vanadium shale. In this way, vanadium and the main valuable elements, Cr and Na, in the leaching solution can be recovered stepwise, which can reduce the production cost and environmental pollution.

Acknowledgments

The authors are grateful for the financial supports from the National Key Research and Development Program of China (No. 2020YFC1909700), and the National Natural Science Foundation of China (Nos. 51974207, 51774215).

References

[1] CHEN Hui, ZHANG Xin-yu, ZHANG Shi-rui, WU Sai-xue, CHEN Fu-yu, XU Jian-guang. A comparative study of iron−vanadium and all-vanadium flow battery for large scale energy storage [J]. Chemical Engineering Journal, 2022, 429: 132403.

[2] CHEN Bo, BAO Shen-xu, ZHANG Yi-min. Synergetic strengthening mechanism of ultrasound combined with calcium fluoride towards vanadium extraction from low-grade vanadium-bearing shale [J]. International Journal of Mining Science and Technology, 2021, 31(6): 1095−1106.

[3] BHATTACHARJEE A, SAHA H. Development of an efficient thermal management system for vanadium redox flow battery under different charge−discharge conditions [J]. Applied Energy, 2018, 230: 1182−1192.

[4] HUANG Ze-bo, MU An-le, WU Long-xing, WANG Hang, ZHANG Yong-jun. Electrolyte flow optimization and performance metrics analysis of vanadium redox flow battery for large-scale stationary energy storage [J]. International Journal of Hydrogen Energy, 2021, 46(63): 31952−31962.

[5] LI Hong-yi, CHEN Xin-mian, LI Dan-qing, GUO Yun, DIAO Jiang, XIE Bing. Quick valence analysis method of vanadium toward accurate toxicity assessment of vanadium-containing hazardous wastes [J]. Transactions of Nonferrous Metals Society of China, 2021, 31(11): 3602−3612.

[6] WANG Xue-wen, YANG Ming-e, MENG Yu-qi, GAO Da-xiong, WANG Ming-yu, FU Zi-bi. Cyclic metallurgical process for extracting V and Cr from vanadium slag: Part I. Separation and recovery of V from chromium-containing vanadate solution [J]. Transactions of Nonferrous Metals Society of China, 2021, 31(3): 807−816.

[7] LI Xing-bin, DENG Zhi-gan, WEI Chang, LI Cun-xiong, LI Min-ting, FAN Gang, HUANG Hui. Solvent extraction of vanadium from a stone coal acidic leach solution using D2EHPA/TBP: Continuous testing [J]. Hydrometallurgy, 2015, 154: 40−46.

[8] CHEN De-sheng, ZHAO Hong-xin, HU Guo-ping, QI Tao, YU Hong-dong, ZHANG Guo-zhi, WANG Li-na, WANG Wei-jing. An extraction process to recover vanadium from low-grade vanadium-bearing titanomagnetite [J]. Journal of Hazardous Materials, 2015, 294: 35−40.

[9] NGUYEN T H, LEE M S. Solvent extraction of vanadium (V) from sulfate solutions using LIX 63 and PC 88A [J]. Journal of Industrial and Engineering Chemistry, 2015, 31: 118−123.

[10] LI Xing-bin, WEI Chang, WU Jun, LI Min-ting, DENG Zhi-gan, LI Cun-xiong, XU Hong-sheng. Co-extraction and selective stripping of vanadium (IV) and molybdenum (VI) from sulphuric acid solution using 2-ethylhexyl phosphonic acid mono-2-ethylhexyl ester [J]. Separation and Purification Technology, 2012, 86: 64−69.

[11] TAVAKOLI M R, DREISINGER D B. Separation of vanadium from iron by solvent extraction using acidic and neutral organophosporus extractants [J]. Hydrometallurgy, 2014, 141: 17−23.

[12] WEN Jia-wei, NING Peng-ge, CAO Hong-bin, SUN Zhi, ZHANG Yi, XU Gao-jie. Recovery of high-purity vanadium from aqueous solutions by reusable primary amines N1923 associated with semiquantitative understanding of vanadium species [J]. ACS Sustainable Chemistry & Engineering, 2018, 6(6): 7619−7626.

[13] JING Xiao-hua, WU Zhi-neng, DU Ji-min, WANG Xiao-jin, JING Xiao-dong. Kinetics of V(V) extraction in V(V)−SO_4^{2-} (Na^+, H^+)−primary amine N1923-sulfonated kerosene system using single drop technique [J]. Separation and Purification Technology, 2019, 215: 473−479.

[14] QIN Zhi-feng, ZHANG Guo-quan, XIONG Ying-jie, LUO Dong-mei, LI Chun. Recovery of vanadium from leach solutions of vanadium slag using solvent extraction with N235 [J]. Hydrometallurgy, 2020, 192: 105259.

[15] YE Guo-hua, HU Yi-bo, TONG Xiong, LU Lu. Extraction of vanadium from direct acid leaching solution of clay vanadium ore using solvent extraction with N235 [J]. Hydrometallurgy, 2018, 177: 27−33.

[16] ZHANG Ying, ZHANG Ting-an, DREISINGER D, ZHOU Wei-hua, XIE Feng, LV Guo-zhi, ZHANG Wei-guang. Chelating extraction of vanadium (V) from low pH sulfuric acid solution by Mextral 973H [J]. Separation and Purification Technology, 2018, 190: 123−135.

[17] LIU Yuan, LI Qing-gang, ZHANG Tao, WU Xin-sheng, DU Jia-wei, ZHANG Gui-qing, ZENG Li. New process consisting of oxidative stripping of vanadium from loaded D2EHPA organic solution with H_2O_2 and direct precipitation with sulfuric acid [J]. Hydrometallurgy, 2021, 203: 105611.

[18] HU Guo-ping, CHEN De-sheng, WANG Li-na, LIU Jing-chong, ZHAO Hong-xin, LIU Ya-hui, QI Tao, ZHANG Chang-qiao, YU Ping. Extraction of vanadium from chloride solution with high concentration of iron by solvent extraction using D2EHPA [J]. Separation and Purification Technology, 2014, 125: 59−65.

[19] CHEN Bian-fang, HUANG Sheng, LIU Biao, GE Qi, XIE Shu-shan, WANG Ming-yu, WANG Xue-wen. Thermodynamic analysis for separation of vanadium and chromium in V(IV)−Cr(III)−H_2O system [J]. Transactions of Nonferrous Metals Society of China, 2018, 28(3): 567−573.

[20] SHEN Chun, ZHANG Yi-min, HUANG Jing, BAO Shen-xu, YANG Xiao, XIONG Pu. Separation of vanadium (V) using N235 by three-phase system in concentrated HCl media [J]. Canadian Journal of Chemistry, 2017, 95(6): 717−722.

[21] ZHANG Guo-zhi, CHEN De-sheng, ZHAO Wei, ZHAO Hong-xin, WANG Li-na, LI Dan, QI Tao. A novel synergistic extraction method for recovering vanadium (V) from high-acidity chloride leaching liquor [J]. Separation and Purification Technology, 2016, 165: 166−172.

[22] LIU Hong, ZHANG Yi-min, HUANG Jing, LIU Tao, XUE Nan-nan, WANG Kui. Selective separation and recovery of vanadium from a multiple impurity acid leaching solution of stone coal by emulsion liquid membrane using di-(2-ethylhexyl)phosphoric acid [J]. Chemical Engineering Research and Design, 2017, 122: 289−297.

[23] SHIN K H, JIN C S, SO J Y, PARK S K, KIM D H, YEON S H. Real-time monitoring of the state of charge (SOC) in vanadium redox-flow batteries using UV−Vis spectroscopy in operando mode [J]. Journal of Energy Storage, 2020, 27: 101066.

[24] MIRANDA C T, CARVALHO S, YAMAKI R T, PANIAGO E B, BORGES R H U, de BELLIS V M. pH-metric, UV–Vis and ^{51}V NMR study of vanadium (V) coordination to α-aminohydroxamic acids in aqueous solutions [J]. Polyhedron, 2010, 29: 897−903.

[25] LIU Hong, ZHANG Yi-min, HUANG Jing. Separation and transfer mechanism of vanadium from black shale leaching solution by supported liquid membrane using N235 [J]. The Chinese Journal of Nonferrous Metals, 2020, 30(9): 2216−2223. (in Chinese)

[26] YING Zi-wen, HUO Man-xing, WU Gui-xuan, LI Jie, JU Yun, WEI Qi-feng, REN Xiu-lian. Recovery of vanadium and chromium from leaching solution of sodium roasting vanadium slag by stepwise separation using amide and EHEHPA [J]. Separation and Purification Technology, 2021, 269: 118741.

[27] RAZAVI S, HAGHTALAB A, KHANCHI A. Thermo-dynamic modeling of the solvent extraction equilibrium for the recovery of vanadium (V) from acidic sulfate solutions using di-(2-ethylhexyl) phosphoric acid [J]. Fluid Phase Equilibria, 2018, 474: 20−31.

[28] LIU Cong, LIU Tao, ZHANG Yi-min, DAI Zi-lin, YANG Ya-dong. Preparation of electrolyte for vanadium redox flow battery from sodium−polyvanadate precipitated wastewater [J]. Separation and Purification Technology, 2020, 240: 116582.

[29] SHI Qi-hua, ZHANG Yi-min, HUANG Jing, LIU Tao, LIU Hong, WANG Lu-yao. Synergistic solvent extraction of vanadium from leaching solution of stone coal using D2EHPA and PC88A [J]. Separation and Purification Technology, 2017, 181: 1−7.

[30] ZHANG Ying, ZHANG Ting-an, LV Guo-zhi, ZHANG Guo-quan, LIU Yan. Synergistic extraction of vanadium (IV) in sulfuric acid media using a mixture of D2EHPA and EHEHPA [J]. Hydrometallurgy, 2016, 166: 87−93.

[31] DING Mu-qing, LIU Tao, ZHANG Yi-min. Investigations of the influences of K^+ impurity on the electrolyte for vanadium redox flow battery [J]. Ionics, 2020, 26(7): 3415−3423.

[32] ZHANG Z H, WEI L, WU M C, BAI B F, ZHAO T S. Chloride ions as an electrolyte additive for high performance vanadium redox flow batteries [J]. Applied Energy, 2021, 289: 116690.

[33] LI Li-yu, KIM S H, WANG Wei, VIJAYAKUMAR M, NIE Zi-min, CHEN Bao-wei, ZHANG Jian-lu, XIA Guan-guang, HU Jian-zhi, GRAFF G, LIU Jun, YANG Zhen-guo. A stable vanadium redox-flow battery with high energy density for large-scale energy storage [J]. Advanced Energy Materials, 2011, 1(3): 394−400.

[34] REED D, THOMSEN E, LI Bin, WANG Wei, NIE Zi-min, KOEPPEL B, SPRENKLE V. Performance of a low cost interdigitated flow design on a 1 kW class all vanadium mixed acid redox flow battery [J]. Journal of Power Sources, 2016, 306: 24−31.

[35] SHI Yue-yue, XIONG Da-zhen, ZHAO Yang-yang, LI Tie-mei, ZHANG Kai-ge, FAN Jing. Highly efficient extraction/separation of Cr (VI) by a new family of hydrophobic deep eutectic solvents [J]. Chemosphere, 2020, 241: 125082.

[36] BERKESSA Y, LANG Qiao-lin, YAN Bing-hua, KUANG Shao-ping, MAO De-bin, SHU Li, ZHANG Yang. Anion exchange membrane organic fouling and mitigation in salt valorization process from high salinity textile wastewater by bipolar membrane electrodialysis [J]. Desalination, 2019, 465: 94−103.

[37] ZHAO Sheng-xin, CHEN Zhong-lin, SHEN Ji-min, KANG Jing, QU Yan-feng, WANG Bin-yuan, WANG Xin, YUAN Lie. Response surface methodology investigation into optimization of the removal condition and mechanism of Cr(VI) by Na_2SO_3/CaO [J]. Journal of Environmental Management, 2017, 202: 38−45.

[38] ZHANG Qiang, GAO Jing, QIU Yun-ren. Removal of Ni(II) and Cr(III) by complexation-ultrafiltration using rotating disk membrane and the selective separation by shear induced dissociation [J]. Chemical Engineering and Processing: Process Intensification, 2019, 135: 236−244.

[39] YANG Ming-e, YANG Hao-xiang, TIAN Sheng-hui, WANG Ming-yu, WANG Xue-wen. Cyclic metallurgical process for extracting V and Cr from vanadium slag: Part II. Separation and recovery of Cr from vanadium precipitated solution [J]. Transactions of Nonferrous Metals Society of China, 2021, 31(9): 2852−2860.

D2EHPA 萃取法从钒页岩高氯浸出液中制备钒电解液

刘 红[1,2,3,4]，张一敏[1,2,3,4]，刘 涛[1,2,3,4]，黄 晶[1,2,3,4]，陈黎明[1,2,3,4]，胡幼文[1,2,3,4]

1. 武汉科技大学 资源与环境工程学院，武汉 430081；
2. 武汉科技大学 国家环境保护矿冶资源利用与污染控制重点实验室，武汉 430081；
3. 武汉科技大学 钒资源高效利用湖北省协同创新中心，武汉 430081；
4. 武汉科技大学 湖北省页岩钒资源高效清洁利用工程技术研究中心，武汉 430081

摘 要：提出一种从钒页岩中回收有价元素并制备钒电解液的工艺。结果表明，在料液 pH 值为 2.6、萃取剂 D2EHPA 浓度为 20%、相比(O/A)为 1:1、萃取时间为 8 min、H_2SO_4 浓度为 4 mol/L 及反萃时间为 30 min 的条件下，钒萃取率为 99.3%，反萃率为 99.8%。对制备的电解液组成及电化学性能进行详细研究。溶液化学和红外光谱分析表明，浸出液中氯离子可以与钒离子络合，促进钒的萃取。采用本研究提出的工艺能实现钒页岩的综合利用，并避免钒电解液制备过程中有害物质对环境的潜在污染。

关键词：钒页岩；溶剂萃取；钒电解液；电化学性能

(Edited by Wei-ping CHEN)